Supporting Information

Table of Contents

1. Compound Overview

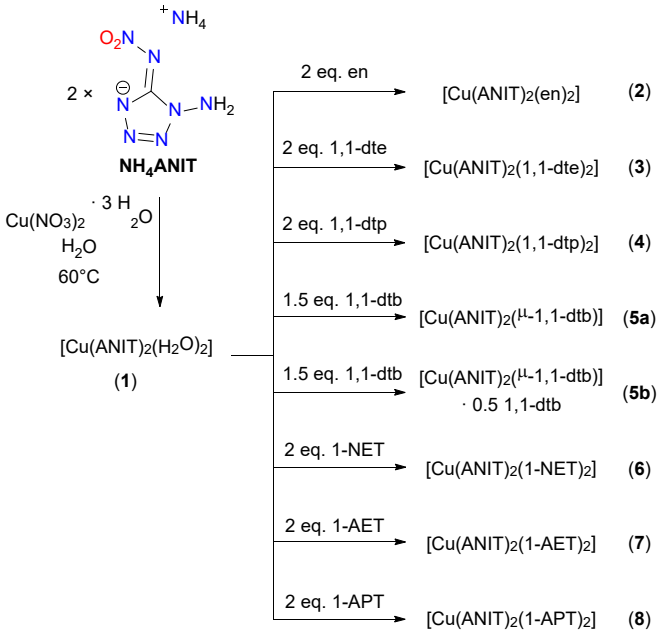

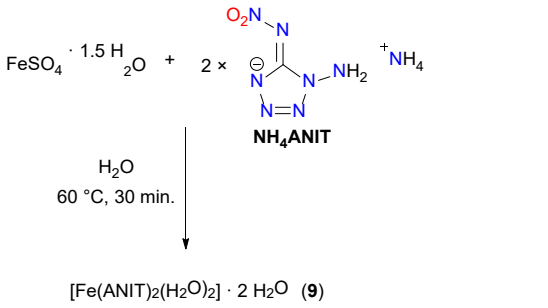

2. Single Crystal X-Ray Diffraction

For all crystalline compounds an Oxford Xcalibur3 diffractometer with a CCD area detector or Bruker D8 Venture TXS diffractometer equipped with a multilayer monochromator, a Photon 2 detector, and a rotating-anode generator were employed for data collection using Mo-Kα radiation (λ = 0.7107 Å). On the Oxford device, data collection and reduction were carried out using the CrysAlisPRO software.[S1] On the Bruker diffractometer, the data were collected with the Bruker Instrument Service v3.0.21, the data reduction was performed using the SAINT V8.18C software (Bruker AXS Inc., 2011). The structures were solved by direct methods (SHELXT[S2]), refined by full-matrix least-squares on *F2* (SHELXL[S3]) and finally checked using the PLATON software[S4] integrated in the WinGX[S2],[S5] or Olex2[S6] software suite. The non-hydrogen atoms were refined anisotropically and the hydrogen atoms were located and freely refined. The absorptions were corrected by a SCALE3 ABSPACK or SADABS Bruker APEX3 multi-scan method.[S7],[S8] All DIAMOND4[S9] plots are shown with thermal ellipsoids at the 50% probability level and hydrogen atoms are shown as small spheres of arbitrary radius.

Table S 1. Crystallographic data and crystal structure refinement details of compounds **1**, **3** and **4**.

	$[Cu(ANIT)_2(H_2O)_2]$	$[Cu(ANIT)_2(1,1\text{-}dte)_2]$	$[Cu(ANIT)_2(1,1\text{-}dtp)_2]$
Formula	$C_2H_8CuN_{14}O_6$	$C_{10}H_{16}CuN_{30}O_4$	$C_{12}H_{20}CuN_{30}O_4$
FW [g mol^{-1}]	387.76	684.07	712.12
Crystal system	monoclinic	monoclinic	triclinic
Space group	$P2_1/n$ (No. 14)	$P2_1/c$ (No. 14)	$P\bar{1}$ (No. 2)
Color / Habit	Green Block	Blue Block	Blue Block
Size [mm]	0.08 x 0.10 x 0.20	0.06 x 0.10 x 0.20	0.10 x 0.40 x 0.50
a [Å]	5.605(3)	8.5508(2)	7.1719(5)
b [Å]	9.087(6)	11.3930(3)	8.6415(6)
c [Å]	11.608(7)	12.2836(3)	10.9893(9)
α [°]	90	90	81.323(6)
β [°]	95.790(12)	93.955(1)	77.233(6)
γ [°]	90	90	86.399(6)
V [Å^3]	588.2(6)	1193.81(5)	656.33(9)
Z	2	2	1
$\rho_{calc.}$ [g cm^{-3}]	2.19	1.903	1.802
μ [mm^{-1}]	1.93	1.009	0.922
F(000)	390	694	363
$\lambda_{MoK\alpha}$ [Å]	0.71073	0.71073	0.71073
T [K]	173	173	123
θ Min-Max [°]	3.5, 36.3	3.0, 33.2	1.9, 26.4
Dataset	−9: 9; −15: 15; −19: 19	−13: 13; −17: 17; −18: 18	−8: 8; −7: 10; −13: 13
Reflections collected	18072	33006	4779
Independent refl.	2861	4565	2631
R_{int}	0.034	0.064	0.049
Observed reflections	2539	3707	2256
Parameters	120	237	222
R_1 (obs)[a]	0.0262	0.034	0.0507
wR_2 (all data)[b]	0.069	0.0826	0.1419
S [c]	1.09	1.05	1.04
Resd. dens [e Å^{-3}]	−0.37, 0.48	−0.52, 0.35	−0.74, 0.94
Absorption correction	multi-scan	multi-scan	multi-scan
CCDC	2394591	2394593	2394588

[a]$R_1 = \Sigma||F_0|-|F_c||/\Sigma|F_0|$; [b]$wR_2 = [\Sigma[w(F_0^2-F_c^2)^2]/\Sigma[w(F_0)^2]]^{1/2}$; $w = [\sigma c^2(F_0^2)+(xP)^2+yP]^{-1}$ and $P=(F_0^2+2F_c^2)/3$; [c]$S = \{\Sigma[w(F_o^2-F_c^2)^2]/(n-p)\}^{1/2}$ (n = number of reflections; p = total number of parameters).

Table S 2. Crystallographic data and crystal structure refinement details of compounds **5a**, **5b**, and **7**.

	[Cu(ANIT)$_2$(μ-1,1-dtb)]	[Cu(ANIT)$_2$(μ-1,1-dtb)] · 0.5 1,1-dtb	[Cu(ANIT)$_2$(1-AET)$_2$]
Formula	$C_8H_{14}CuN_{22}O_4$	$C_8H_{14}CuN_{22}O_4$, $C_3H_5N_4$	$C_8H_{14}CuN_{28}O_4$
FW [g mol^{-1}]	545.95	643.06	630.01
Crystal system	triclinic	triclinic	triclinic
Space group	*P*−1 (No. 2)	*P*−1 (No. 2)	*P*−1 (No. 2)
Color / Habit	Blue Block	Blue Needle	Blue Plate
Size [mm]	0.05 x 0.15 x 0.15	0.01 x 0.10 x 0.50	0.02 x 0.06 x 0.12
a [Å]	7.5130(5)	8.5054(5)	7.6635(3)
b [Å]	10.4994(6)	9.3145(6)	8.3252(3)
c [Å]	13.9744(10)	16.4303(10)	8.8503(3)
α [°]	90.076(5)	73.794(5)	94.183(1)
β [°]	104.597(6)	78.909(5)	93.961(1)
γ [°]	110.881(6)	80.601(5)	92.207(1)
V [Å^3]	991.61(12)	1218.27(13)	561.26(4)
Z	2	2	1
$\rho_{calc.}$ [g cm^{-3}]	1.829	1.753	1.864
μ [mm^{-1}]	1.178	0.978	1.062
F(000)	554	656	319
$\lambda_{MoK\alpha}$ [Å]	0.71073	0.71073	0.71073
T [K]	123	123	173
θ Min-Max [°]	2.1, 32.6	2.3, 31.9	3.2, 30.5
Dataset	−10: 10; −14: 15; −21: 15	−12: 12; −11: 13; −23: 22	−10: 10; −11: 11; −12: 12
Reflections collected	11878	13732	16193
Independent refl.	6501	7379	3413
R_{int}	0.033	0.043	0.039
Observed reflections	4682	5249	3053
Parameters	335	395	215
R_1 (obs)[a]	0.0464	0.05	0.0319
wR_2 (all data)[b]	0.1041	0.1016	0.0728
S [c]	1.03	1.04	1.08
Resd. dens [e Å^{-3}]	−0.56, 0.99	−0.53, 0.56	−0.37, 0.40
Absorption correction	multi-scan	multi-scan	multi-scan
CCDC	2394623	2394590	2394592

[a]$R_1 = \Sigma||F_0|-|F_c||/\Sigma|F_0|$; [b]$wR_2 = [\Sigma[w(F_0^2-F_c^2)^2]/\Sigma[w(F_0)^2]]^{1/2}$; $w = [\sigma c^2(F_0^2)+(xP)^2+yP]^{-1}$ and $P=(F_0^2+2F_c^2)/3$; [c]$S = \{\Sigma[w(F_o^2-F_c^2)^2]/(n-p)\}^{1/2}$ (n = number of reflections; p = total number of parameters).

Table S 3. Crystallographic data and crystal structure refinement details of compounds **1**, **3** and **4**.

	$[Cu(ANIT)_2(1\text{-}APT)_2]$	$[Fe(ANIT)_2(H_2O)_2] \cdot 2\ H_2O$
Formula	$C_{10}H_{18}CuN_{28}O_4$	$C_2H_8FeN_{14}O_6$, $2(H_2O)$
FW [g mol^{-1}]	658.06	416.11
Crystal system	monoclinic	triclinic
Space group	$P2_1/n$ (No. 14)	$P\bar{1}$ (No. 2)
Color / Habit	Violet Block	Yellow Plate
Size [mm]	0.15 x 0.20 x 0.25	0.02 x 0.10 x 0.12
a [Å]	11.4578(7)	6.4691(4)
b [Å]	5.8393(4)	6.9872(4)
c [Å]	18.8934(13)	8.3330(5)
α [°]	90	74.463(2)
β [°]	92.536(6)	71.796(2)
γ [°]	90	86.373(2)
V [Å^3]	1262.84(14)	344.65(4)
Z	2	1
$\rho_{calc.}$ [g cm^{-3}]	1.731	2.005
μ [mm^{-1}]	0.948	1.177
F(000)	670	212
$\lambda_{MoK\alpha}$ [Å]	0.71073	0.71073
T [K]	123	173
θ Min-Max [°]	2.0, 32.8	2.7, 29.6
Dataset	−16: 16; −8: 8; −28: 28	−8: 8; −9: 9; −11: 11
Reflections collected	14870	8421
Independent refl.	4314	1924
R_{int}	0.045	0.034
Observed reflections	3095	1836
Parameters	204	139
R_1 (obs)[a]	0.0422	0.0245
wR_2 (all data)[b]	0.1076	0.0609
S [c]	1.04	1.13
Resd. dens [e Å^{-3}]	−0.58, 0.50	−0.40, 0.42
Absorption correction	multi-scan	multi-scan
CCDC	2394589	2394622

[a]$R_1 = \Sigma||F_0|-|F_c||/\Sigma|F_0|$; [b]$wR_2 = [\Sigma[w(F_0^2-F_c^2)^2]/\Sigma[w(F_0)^2]]^{1/2}$; $w = [\sigma c^2(F_0^2)+(xP)^2+yP]^{-1}$ and $P=(F_0^2+2F_c^2)/3$; [c]$S = \{\Sigma[w(F_o^2-F_c^2)^2]/(n-p)\}^{1/2}$ (n = number of reflections; p = total number of parameters).

3. IR Spectroscopy of 1–9

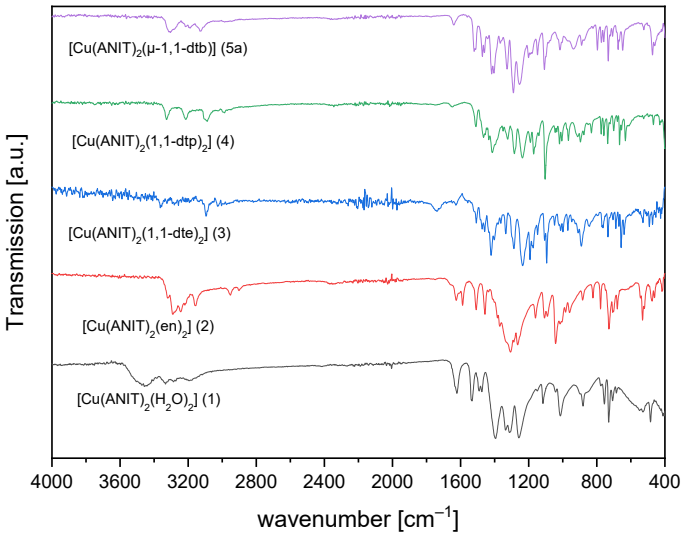

Figure S 1. IR spectra of **1**–**5a**.

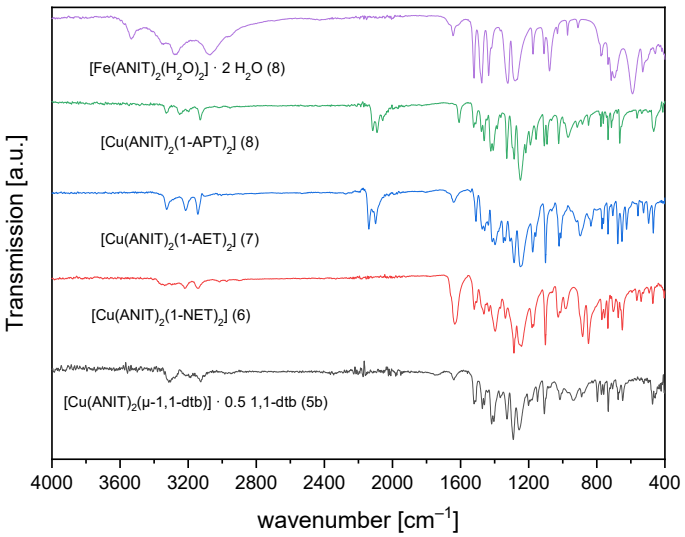

Figure S 2. IR spectra of **5b**–**9**.

4. Thermal analysis of 1–9

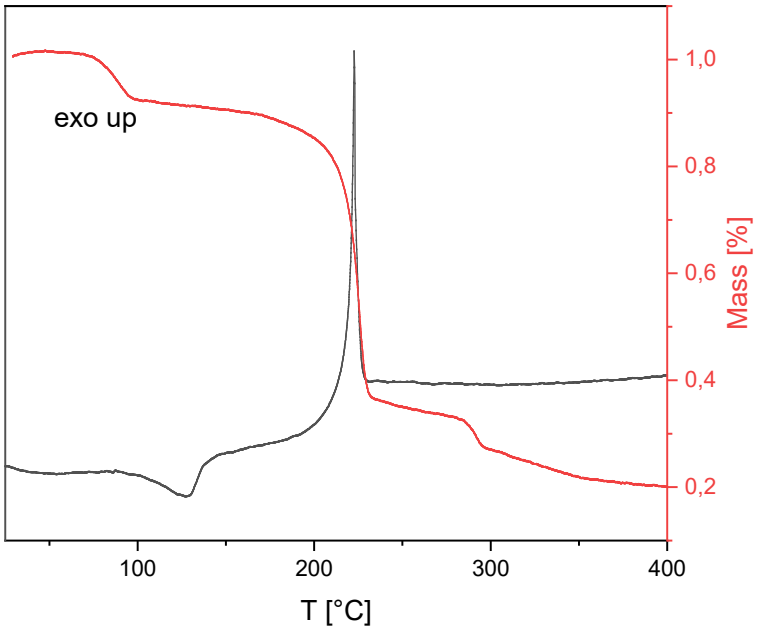

Figure S 3. DTA (black) and TGA (red) plot of $[Cu(ANIT)_2(H_2O)_2]$ (**1**) in the range of 25–400 °C.

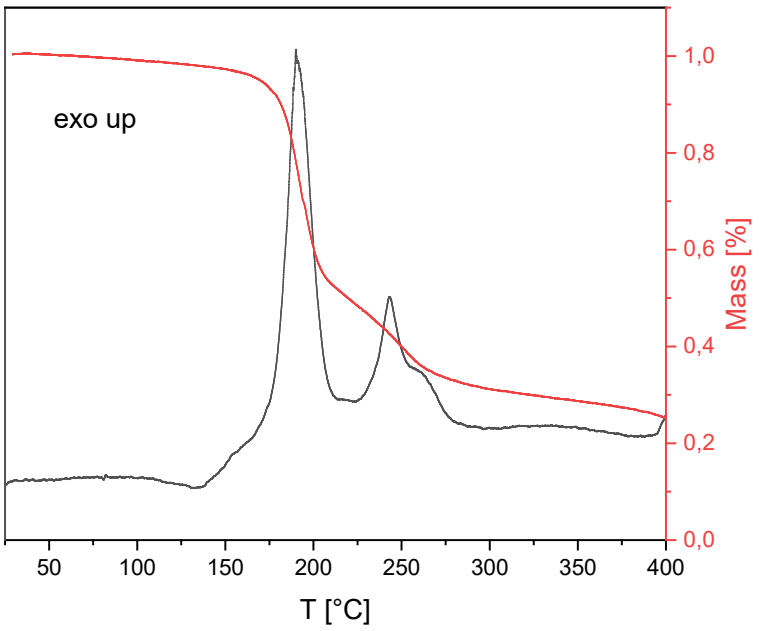

Figure S 4. DTA (black) and TGA (red) plot of $[Cu(ANIT)_2(en)_2]$ (**2**) in the range of 25–400 °C.

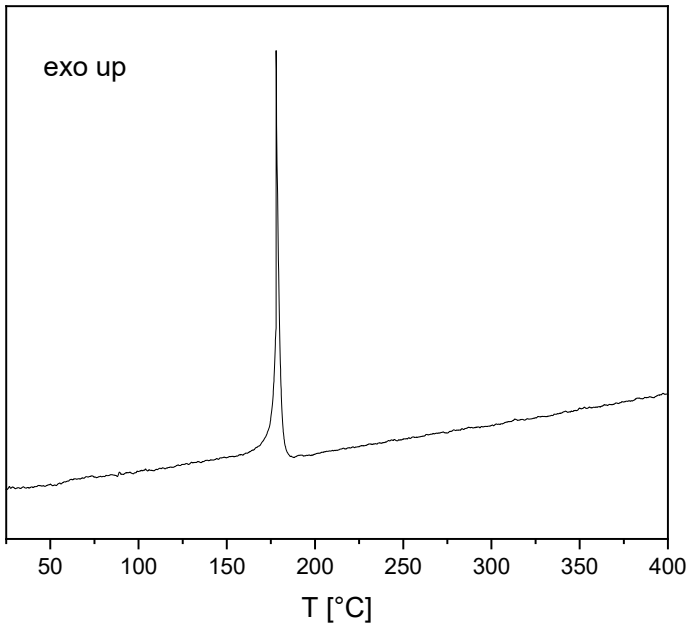

Figure S 5. DTA plot of [Cu(ANIT)$_2$(1,1-dte)$_2$] (**3**) in the range of 25–400 °C.

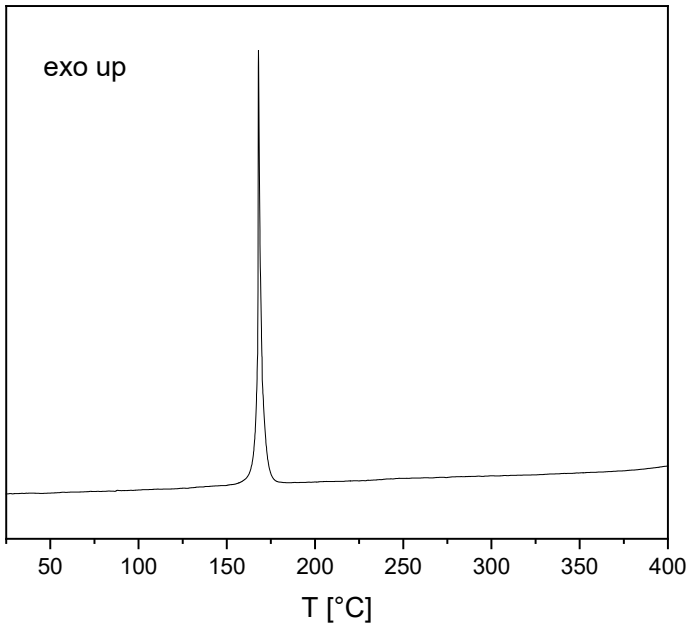

Figure S 6. DTA plot of [Cu(ANIT)$_2$(1,1-dtp)$_2$] (**4**) in the range of 25–400 °C.

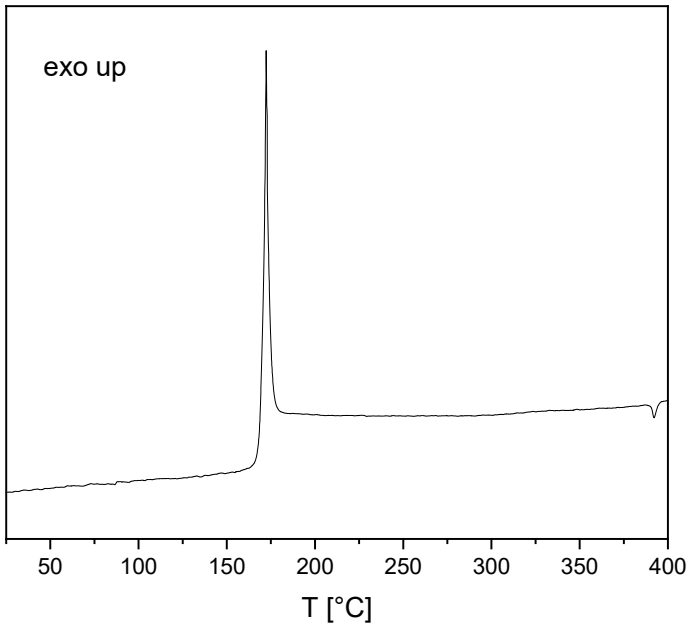

Figure S 7. DTA plot of [Cu(ANIT)$_2$(μ-1,1-dtb)] (**5a**) in the range of 25–400 °C.

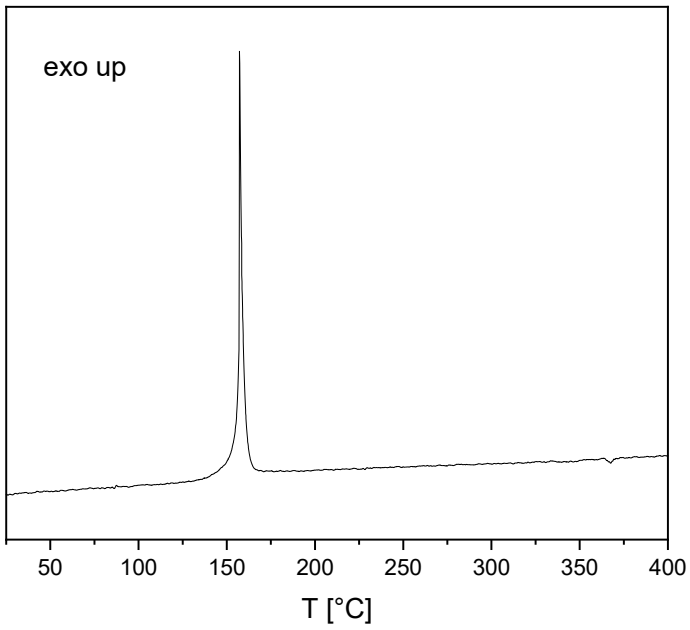

Figure S 8. DTA plot of [Cu(ANIT)$_2$(μ-1,1-dtb)] · 0.5 1,1-dtb (**5b**) in the range of 25–400 °C.

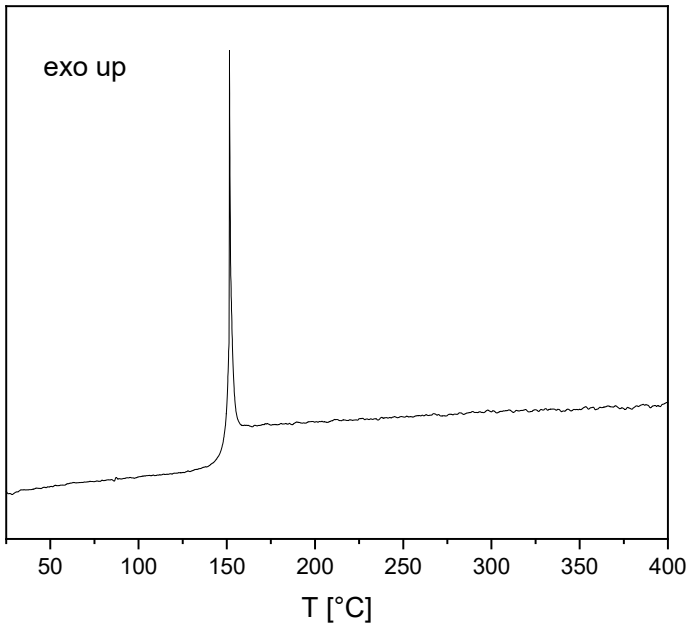

Figure S 9. DTA plot of $[Cu(ANIT)_2(1\text{-}NET)_2]$ (**6**) in the range of 25–400 °C.

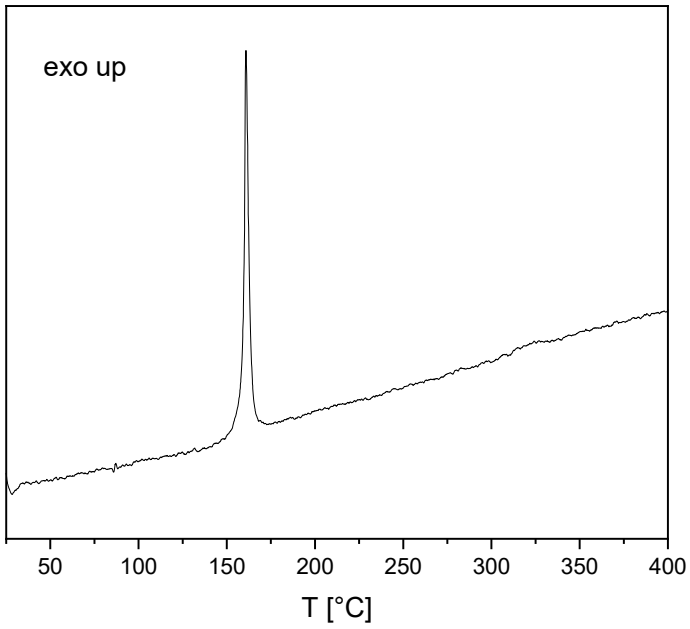

Figure S 10. DTA plot of $[Cu(ANIT)_2(1\text{-}AET)_2]$ (**7**) in the range of 25–400 °C.

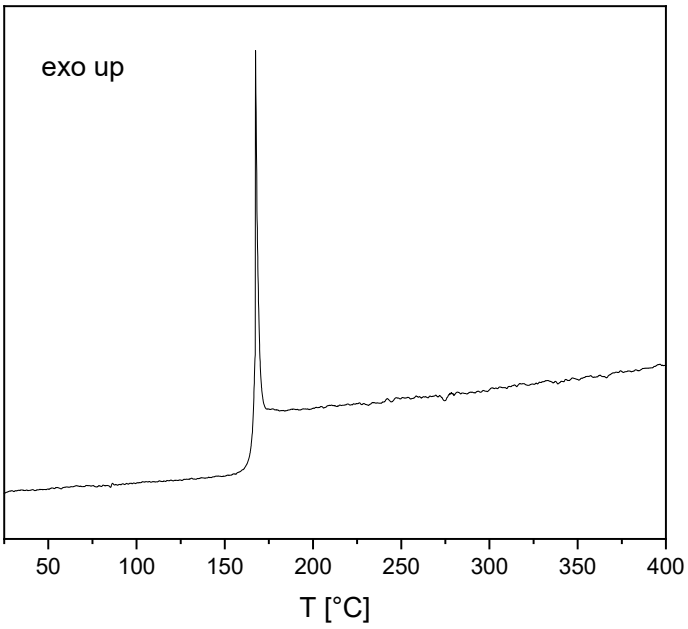

Figure S 11. DTA plot of $[Cu(ANIT)_2(1\text{-}APT)_2]$ (**8**) in the range of 25–400 °C.

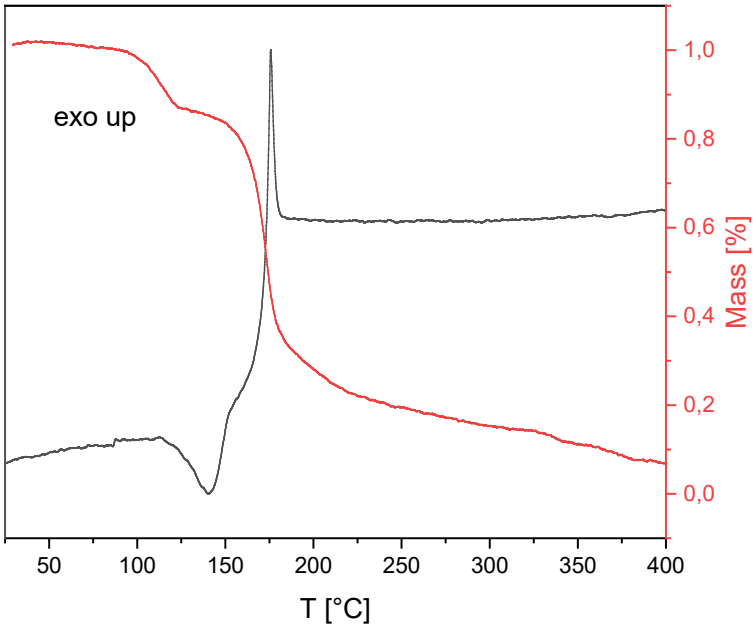

Figure S 12. DTA (black) and TGA (red) plot of $[Fe(ANIT)_2(H_2O)_2] \cdot 2\ H_2O$ (**9**) in the range of 25–400 °C.

5. Hot Plate and Hot Needle Testing

Figure S 13. Hot plate (left) and hot needle test of **1**.

Figure S 14. Hot plate (left) and hot needle test of **2**.

Figure S 15. Hot plate (left) and hot needle test of **3**.

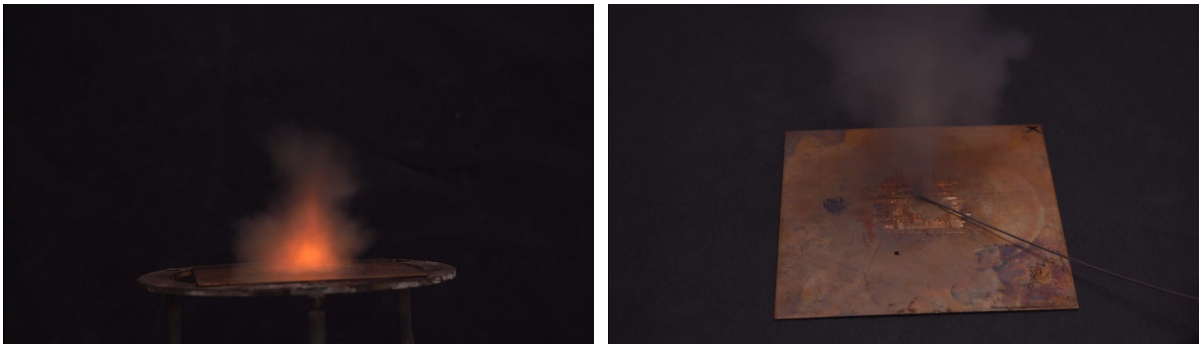

Figure S 16. Hot plate (left) and hot needle test of **4**.

Figure S 17. Hot plate (left) and hot needle test of **5a**.

Figure S 18. Hot plate (left) and hot needle test of **5b**.

Figure S 19. Hot plate (left) and hot needle test of **6**.

Figure S 20. Hot plate (left) and hot needle test of **7**.

Figure S 21. Hot plate (left) and hot needle test of **8**.

Figure S 22. Hot plate (left) and hot needle test of **9**.

6. Scanning Electron Microscopy

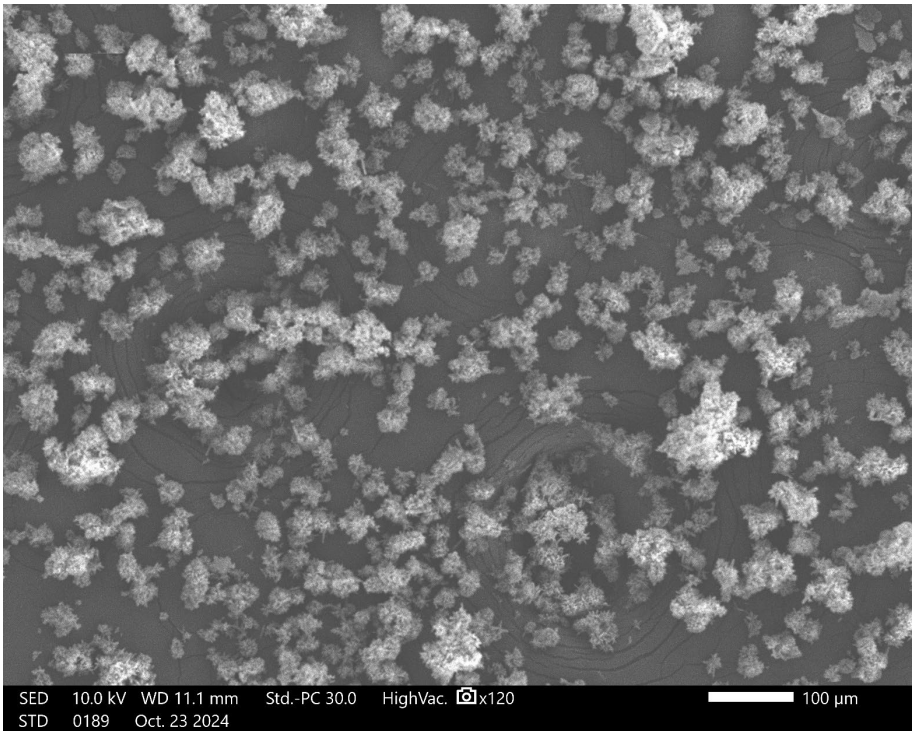

Figure S 23. SEM image of **1** at 120× magnification.

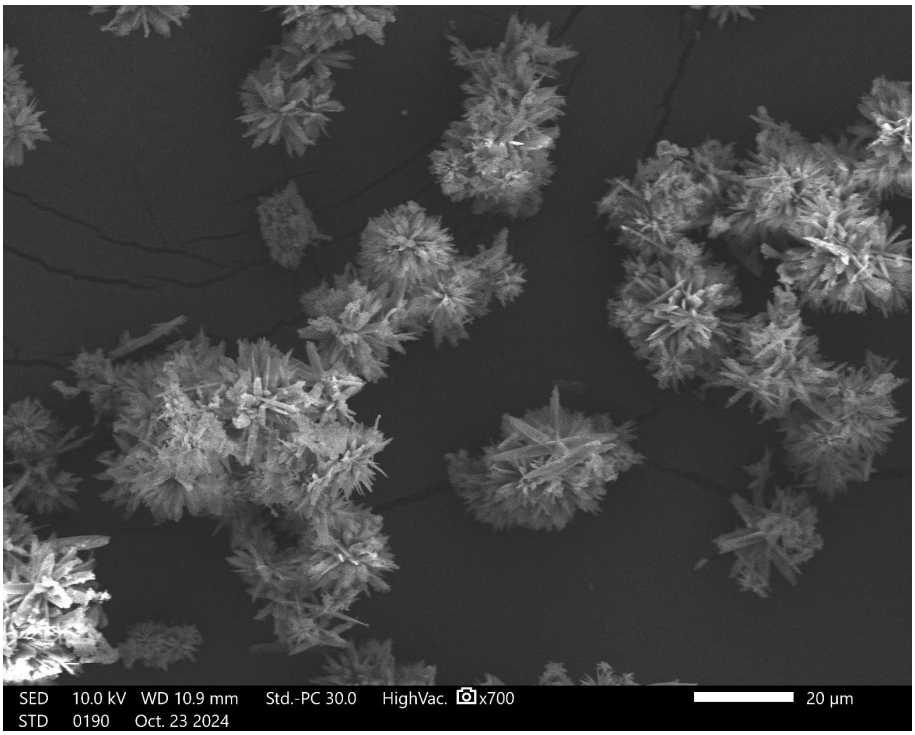

Figure S 24. SEM image of **1** at 700× magnification.

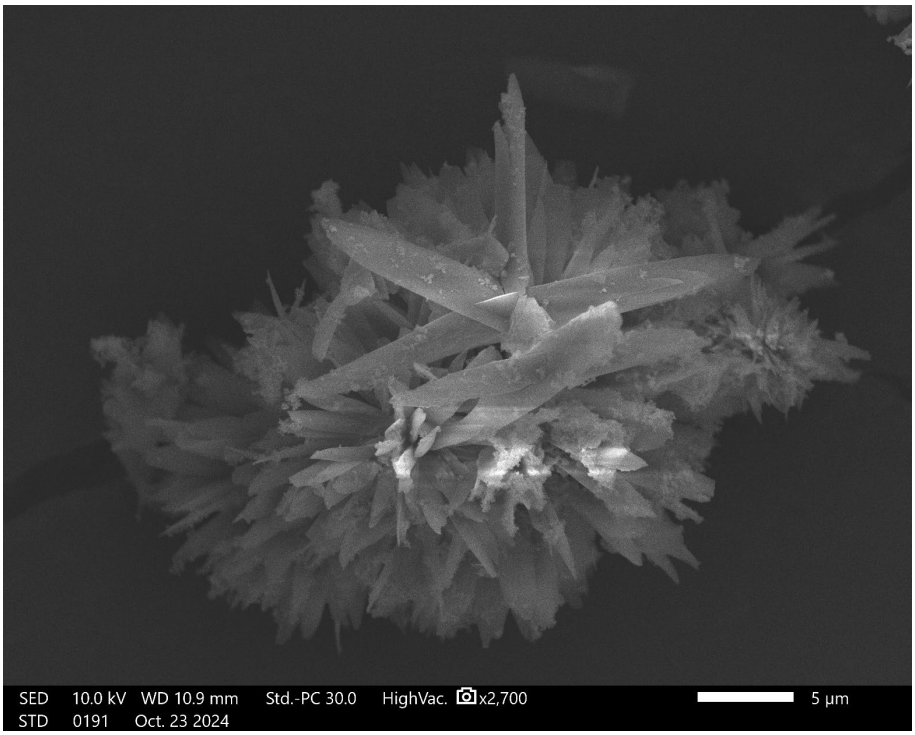

Figure S 25. SEM image of **1** at 2700× magnification.

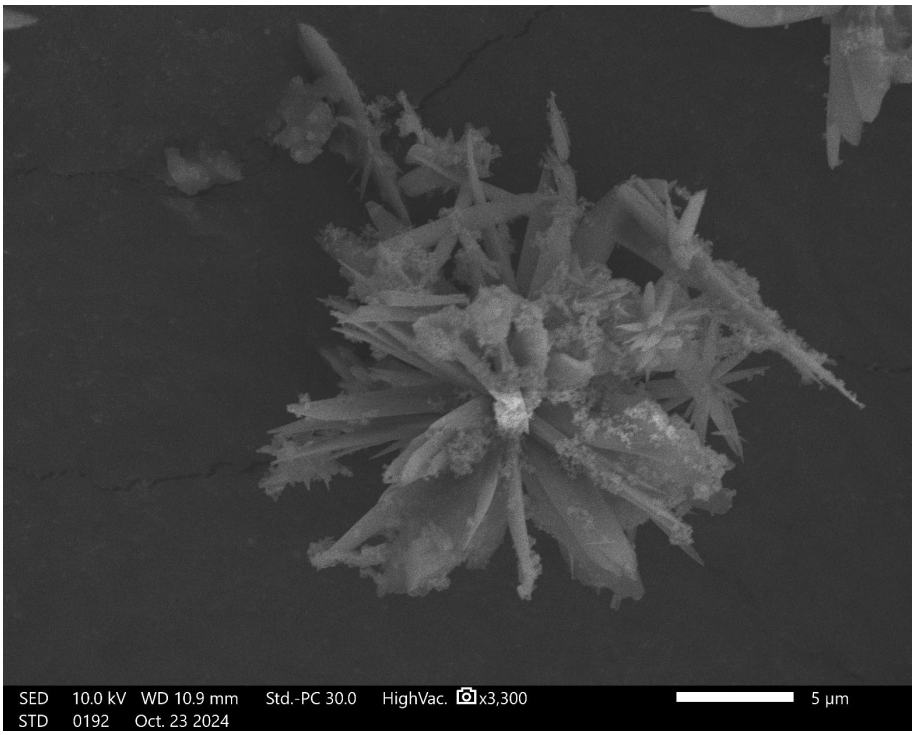

Figure S 26. SEM image of **1** at 3300× magnification.

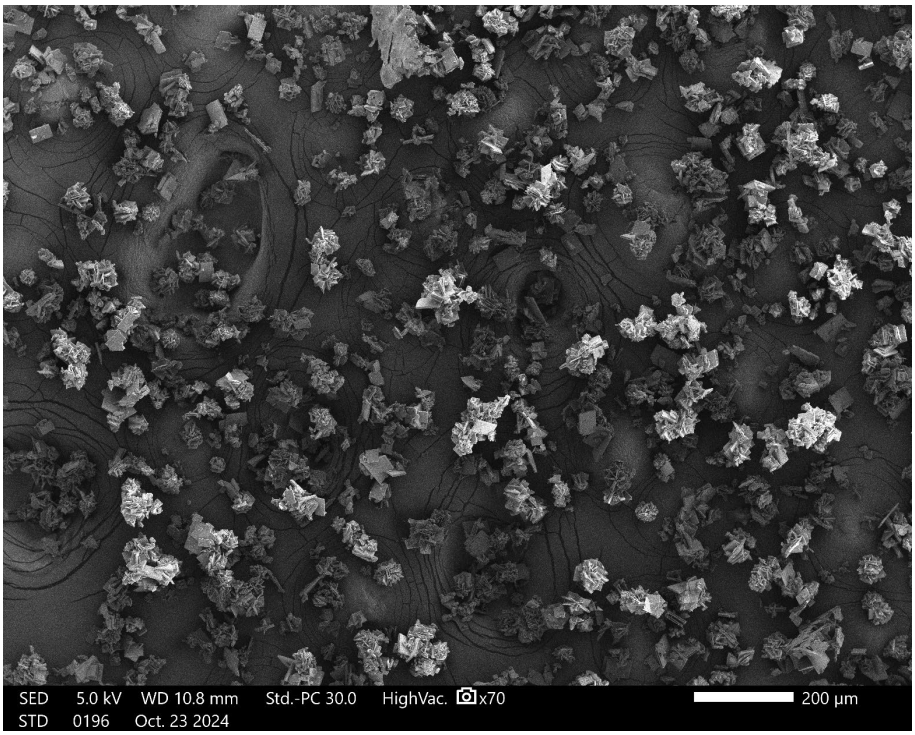

Figure S 27. SEM image of **7** at 70× magnification.

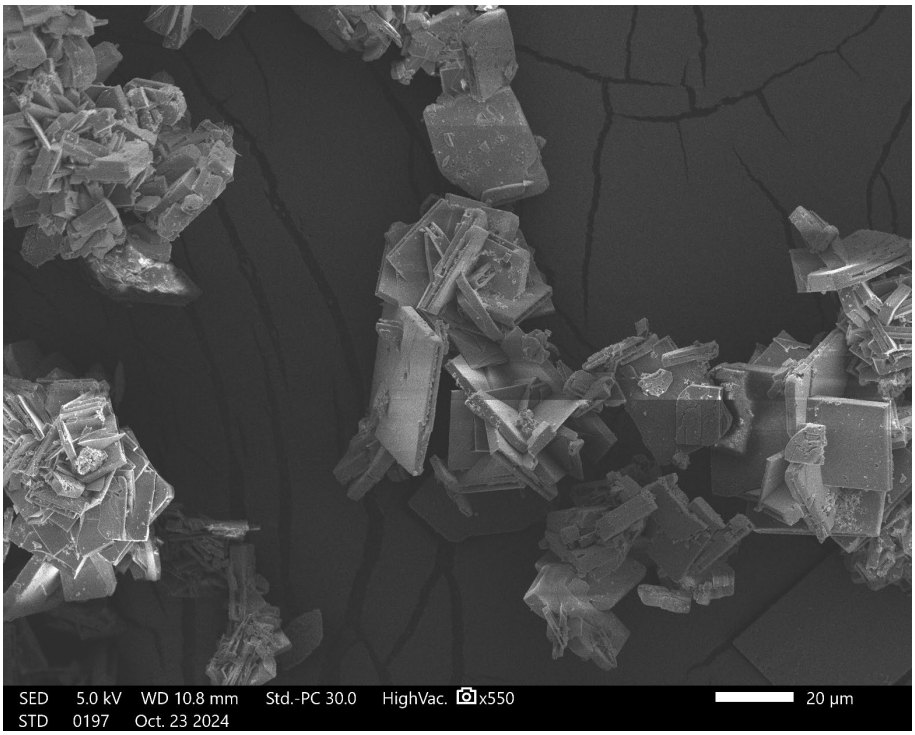

Figure S 28. SEM image of **7** at 550× magnification.

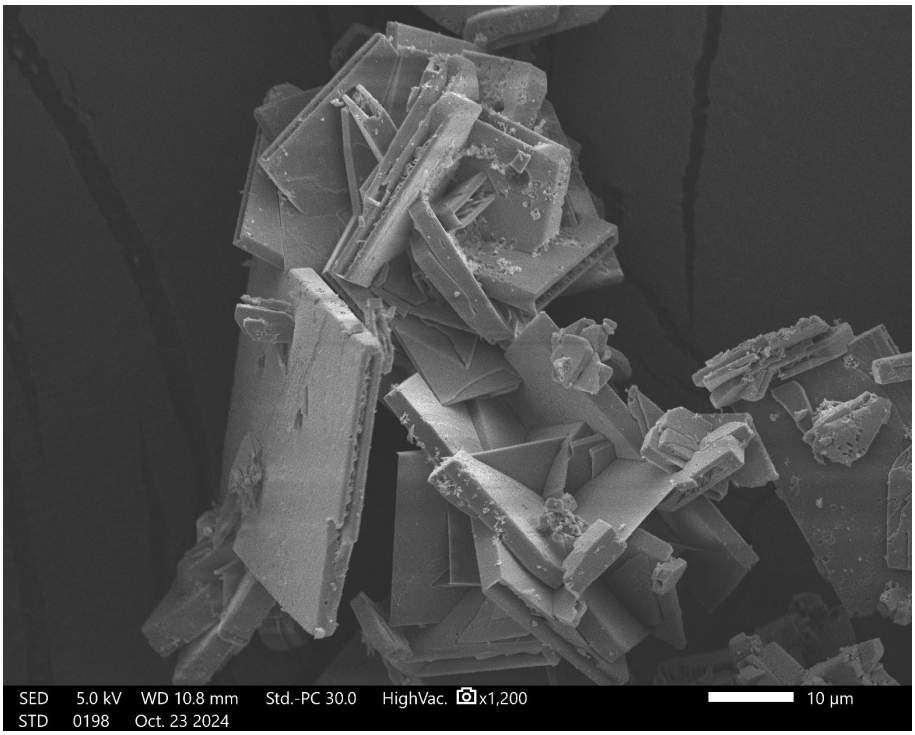

Figure S 29. SEM image of **7** at 1200× magnification.

Figure S 30. SEM image of **7** at 5500× magnification.

7. Experimental and Analytical Methods

All chemicals and solvents were employed as received (Sigma-Aldrich, Fluka, Acros, ABCR). Endothermic and exothermic events of the described compounds, which indicate melting, loss of crystal water or decomposition, are given as the extrapolated onset temperatures. The samples were measured in a range of 25–400 °C at a heating rate of 5 °C min^{-1} through differential thermal analysis (DTA) with an OZM Research DTA 552-Ex instrument. Infrared spectra were measured with pure samples on a Perkin-Elmer BXII FT-IR system with a Smith DuraSampler IR II diamond ATR. Determination of the carbon, hydrogen, and nitrogen contents was carried out by combustion analysis using an Elementar Vario EI (nitrogen values determined are often lower than the calculated ones' due to their explosive behavior). Impact sensitivity tests were carried out according to STANAG 4489[S10] with a modified instruction[S11] using a BAM (Bundesanstalt für Materialforschung) drophammer.[S12] Friction sensitivity tests were carried out according to STANAG 4487[S13] with a modified instruction[S14] using the BAM friction tester.[S12, 15] The classification of the tested compounds results from the "UN Recommendations on the Transport of Dangerous Goods".[S16] Additionally, all compounds were tested upon the sensitivity toward electrical discharge using the OZM Electric Spark XSpark10 device.[S15] The morphology of selected samples was determined by a JEOL JSM-IT210 scanning electron microscope (SEM). The samples were gold-coated (Quorum Q 150R ES plus) to hinder electrostatic charging and to increase the conductivity.

8. References

[S1] *CrysAlisPRO*, Version 171.33.41, Oxford Diffraction Ltd, **2009**.
[S2] G. M. Sheldrick, *Acta Crystallogr. Sect. A* **2015**, *71*, 3–8.
[S3] a) G. M. Sheldrick, *SHELXL-97*, University of Göttingen, Germany, **1997**; b) G. M. Sheldrick, *Acta Crystallogr. Sect. A* **2008**, *64*, 112–122.
[S4] A. L. Spek, *PLATON*, Utrecht University, The Netherlands, **1999**.
[S5] L. J. Farrugia, *J. Appl. Cryst.* **2012**, *45*, 849.
[S6] O. V. Dolomanov, L. J. Bourhis, R. J. Gildea, J. A. K. Howard, H. Puschmann, *J. Appl. Cryst.* **2009**, *42*, 339–341.
[S7] *Empirical absorption correction using spherical harmonics, implemented in SCALE3 ABSPACK scaling algorithm*, Version 171.33.41, CrysAlisPro Oxford Diffraction Ltd., **2009**.
[S8] *APEX3*, Bruker AXS Inc., Madison, Wisconsin, USA,
[S9] H. Putz, K. Brandenburg, *Diamond - Crystal and Molecular Structure Visualization*, Crystal Impact, Bonn, Germany,
[S10] NATO standardization agreement (STANAG) on explosives, impact sensitivity tests, no. 4489, 1st ed., 1999.
[S11] WIWEB-Standardarbeitsanweisung 4–5.1.02, Ermittlung der Explosionsgefährlichkeit, hier der Schlagempfindlichkeit mit dem Fallhammer, According to: **2002**.
[S12] BAM, http://www.bam.de, accessed December 2021.
[S13] NATO standardization agreement (STANAG) on explosive, friction sensitivity tests, no. 4487, According to: 1st. Edition, **2002**.
[S14] WIWEB-Standardarbeitsanweisung 4–5.1.03, Ermittlung der Explosionsgefährlichkeit oder der Reibeempfindlichkeit mit dem Reibeapparat, According to: **2002**.
[S15] OZM, https://www.ozm.cz/, accessed December 2021.
[S16] a) *UN Model Regulation: Recommendations on the Transport of Dangerous Goods – Manual of Tests and Criteria, section 13.4.2.3.3*, **2015**; b) Impact: insensitive > 40 J, less sensitive ≥ 35 J, sensitive ≥ 4 J, very sensitive ≤ 3 J; Friction: insensitive > 360 N, less sensitive = 360 N, sensitive < 360 N and > 80 N, very sensitive ≤ 80 N, extremely sensitive ≤ 10 N, According to: Recommendations on the Transport of Dangerous Goods, Manual of Tests and Criteria, 4th edition, New York-Geneva, **1999**.